

Geochemistry of Kilambo-Kajala and Ilwalilo Hot Springs, Kiejo-Mbaka Geothermal Prospect, Tanzania

Taramaeli Mnjokava^(a), Ariph Kimani^(a), Claudio Pasqua^(b), Matteo Lelli^(b,c), Luigi Marini^(b)

^(a) Tanzania Geothermal Development Company Limited (TGDC), Dar es Salaam, Tanzania; ^(b)ELC-Electroconsult, Milano, Italy; ^(c) IGG-CNR, Pisa, Italy

taramaeli.mnjokava@tanesco.co.tz; ariph.kimani@tanesco.co.tz; claudio.pasqua@elc-electroconsult.com; m.elli@igg.cnr.it; luigimarini@appliedgeochemistry.it

Keywords

Kilambo, Kajala, Ilwalilo, Kiejo, Mbaka

ABSTRACT

The two hot spring groups of Kilambo-Kajala and Ilwalilo are situated along the prominent Mbaka fault, at a distance of ca. 8-9 km one from the other. They represent the outflows of two distinct fault-controlled geothermal circuits. The hot waters discharged in both sites have Na-HCO₃ chemical composition, which is probably acquired through prolonged interaction of meteoric waters with basement rocks (mainly gneisses) sustained by conversion of CO₂ to HCO₃. The undiluted Kilambo-Kajala reservoir liquid has TDS of 4,810 ± 90 mg/L, whereas the pure Ilwalilo reservoir liquid has TDS of ca. 6,000 mg/L. The two liquids have also different ratios between several solutes.

Although maximum outlet temperature is 64 °C in both sites, reservoir temperature is estimated to be 135-139 °C at Kilambo-Kajala and 112-113 °C at Ilwalilo, based on the SiO₂ (quartz/chalcedony) geothermometer, the saturation indices vs. temperature plot, and (for Kilambo-Kajala only) the H₂-Ar and H₂-N₂ gas geothermometers for an R_H of -2.82.

Reservoir P_{CO2} values, 1.74 bar at Kilambo-Kajala and 1.19 bar at Ilwalilo, are two orders of magnitude higher than the corresponding “*full equilibrium P_{CO2} values*”, implying that (i) calcite is stable under reservoir conditions instead of Ca-Al-silicates and (ii) P_{CO2} is an externally fixed parameter. Indeed, the δ¹³C values of CO₂, -5.5 to -6.0 ‰ at Kilambo-Kajala and -5.6 to -6.4 ‰ at Ilwalilo, suggest that CO₂ is mainly contributed by deep sources and a continuous flux of CO₂-rich deep gases passes through the two geothermal systems.

The δ²H and δ¹⁸O values of H₂O indicate that hot spring waters are of meteoric origin, in spite of a negative oxygen shift at Kilambo-Kajala, which is probably due to exchange of O isotopes between H₂O and CO₂. Based on the isotope - elevation relations reconstructed during this

work, recharging meteoric waters infiltrate at average elevation of $1,957 \pm 23$ and $2,186 \pm 5$ m asl for Kilambo-Kajala and Ilwalilo, respectively.

1. Introduction

The geochemical characteristics of waters and gases issued from the hot springs of Kilambo-Kajala and Ilwalilo have been the subject of several studies in the past (SWECO, 1978; Makundi and Kifua, 1985; Pik et al. 2006; Kraml et al., 2008; Delalande et al., 2011; Ochmann and Garofalo 2013; de Moor et al., 2013; Barry et al, 2013) that provided a considerable amount of data.

Recently these two hot spring groups were investigated in the framework of the project "Surface Exploration and Training in Luhoi and Kiejo-Mbaka Geothermal Areas, Tanzania" funded by MFA/ICEIDA that was carried out by TGDC-Tanzania Geothermal Development Company Limited and ELC-Electroconsult. During this survey, eight water samples were collected from carefully selected local cold springs, positioned at different elevations, from 1,200 to 2,800 m asl, to reconstruct the isotope-elevation relations for the area of interest.

In this paper, all available geochemical data are processed and interpreted to provide a contribution for the reconstruction of the conceptual model of the geothermal circuits discharging through the hot springs of Kilambo-Kajala and Ilwalilo.

2. Field Characteristics of the Hot Springs of Kilambo-Kajala and Ilwalilo

The hot springs of Kilambo-Kajala and Ilwalilo are positioned along the NW-trending Mbaka transfer fault system (Figure 1). With a length of ~35 km and a vertical displacement of several hundred meter, the Mbaka transfer fault system represents a tectonic feature of regional importance, also controlling the upflow of the thermal waters towards the surface at Kilambo-Kajala and Ilwalilo.

The hot springs of Ilwalilo are found on the left bank of the Mbaka River, at elevations of ~800 m asl, and distribute over a length of ~150 m. Thermal waters deposit abundant travertine and Fe(III) oxy-hydroxides. Gas emission occurs locally. The total water flowrate is at least 5 L/s and maximum outlet temperature is 64°C.

The hot springs of Kilambo and the hot springs of Kajala are situated along the Nugwisi River, mostly on its left bank, at elevations of ~645-665 m asl and ~610-630 m asl, respectively. The hot springs distribute over a length of ~200 m at Kilambo and ~500 m at Kajala, whereas the distance between the two thermal sites is ~600 m only. Thermal waters deposit abundant travertine, especially at Kilambo, and Fe(III) oxy-hydroxides. Gas emission is copious in both thermal sites. The hot springs of Kilambo and Kajala have total flowrate of ~10 and ~5 L/s, respectively, and maximum outlet temperature of 64 and 59°C, respectively.

As shown in Figure 1, the gas manifestation of Lufundo is found on the footwall block of the Mbaka fault, ~3.5-4.5 km to the N of Kilambo-Kajala. The site is characterized by a high diffuse CO₂ flux from soil, 41.6 ton/day. Other gas emissions (not shown in Figure 1) occur at Kiejo (diffuse CO₂ flux 98.5 ton/day), which is positioned on the SW slopes of Kiejo volcano, ~6 km to the N of Ilwalilo, as well as at Ikama, which is situated along the Mbaka fault zone, ~15 km to the NW of Ilwalilo. Also note that the study area is punctuated by several maars and scoriae cones.

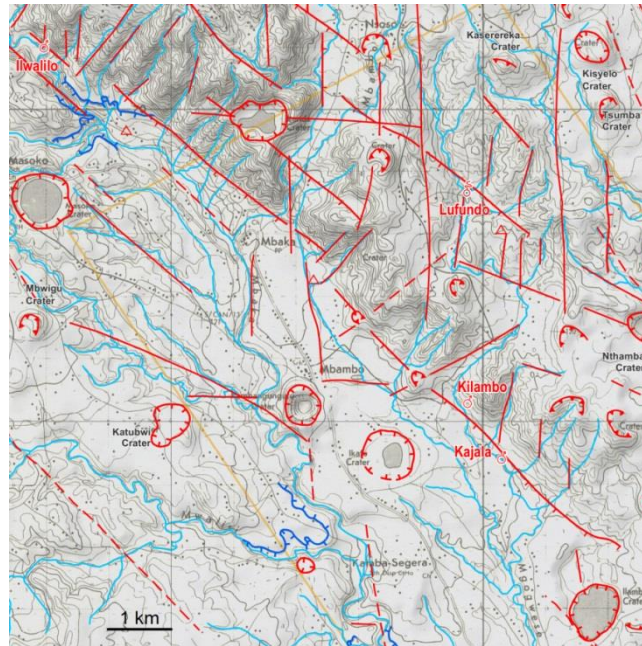


Figure 1: Volcano tectonic map of the study area (from Principe et al. 2017) showing the location of the hot springs of Ilwalilo, Kilambo and Kajala along the NW-trending Mbaka transfer fault system. The Lufundo gas manifestation is positioned on the footwall block of the Mbaka fault. A number of maars (red circles with dashes) and scoriae cones (red circles with triangles) occur in the study area, which is dissected by several faults (red solid lines, dashed if faults are inferred).

3. Sampling and Laboratory Analyses

In October 2016, we collected four water samples plus one gas sample at Kilambo, four water samples plus one gas sample at Kajala, and five water samples plus one gas sample at Ilwalilo. Water temperature, pH, Eh, electrical conductivity, and total alkalinity were measured in the field (results in Table 1) and raw, filtered, filtered-acidified and diluted samples were collected for laboratory analyses. The flowrate of springs (see section 2) was evaluated by multiplying average water velocity times the average cross-section of the channel. Free gas samples were collected both in dry gas bottles and Giggenbach's flasks.

In the IGG-CNR laboratories water samples were analyzed for: (i) Li, Na, K, Mg, Ca, Fe, B, and As by ICP-OES, (ii) SO_4 , Cl, and NO_3 by IC, (iii) F by ISE, and (iv) SiO_2 by UV-Vis, whereas the $\delta^{18}\text{O}$ and $\delta^2\text{H}$ values of H_2O were determined by MS (results in Table 1). The charge unbalance is between -1.8 and +1.0 % for the water samples of the Ilwalilo and Kilambo-Kajala hot springs. Water samples collected from cold springs have charge unbalance between -11.1 and +0.3 %.

Gas samples were analysed for: (i) N_2 , O_2 , Ar, He, H_2 , and CH_4 (>10 ppmv) using a GC with molecular sieve capillary column and a TCD, (ii) CH_4 concentrations (<10 ppmv) by means of the same GC but with a FID, (iii) CO_2 and H_2S utilizing a GC with a packed Chromosorb column and a TCD, and (iv) CO by means of a GC with a molecular sieve column and a RGD (HgO). Wet chemical methods were used to analyse the alkaline solution of the Giggenbach's flasks for H_2S and CO_2 . The $\delta^{13}\text{C}$ value of CO_2 was determined by MS, after standard extraction and purification procedures of the dry gas mixtures and, for samples LF-1 and IL-3, also through acidification of the alkaline solution of the Giggenbach's flasks. The chemical composition of gas mixtures (Table 2) were obtained by merging the analytical results for both dry gas bottles and Giggenbach's flasks. The isotope values of CO_2 are also shown in Table 2.

Code	Place	Easting	Southing	Elevation	Temp.	pH	E.C.	Eh	Na	K	Ca	Mg
		m WGS 84		m asl	°C		µS/cm	mV	mg/L			
KL1	Kilambo	589809	8964958	646	57.6	6.88	5207	-69	1203	62.5	87.2	34.7
KL2	Kilambo	589809	8964958	646	63.3	6.81	5213	-55	1146	62.0	88.5	34.8
KL3	Kilambo	589699	8964927	632	64.0	6.74	5157	-51	1172	63.0	91.5	35.6
KL4	Kilambo	589643	8965050	648	50.1	6.92	5360	-62	1208	67.4	94.4	35.0
KL5	Kajala	590357	8964061	608	58.9	6.66	5130	-64	1161	65.3	63.1	40.9
KL6	Kajala	590485	8964102	609	42.3	6.36	4060	-92	928	51.9	76.9	29.5
KL8	Kajala	590329	8964409	628	55.2	6.75	4916	-88	1088	62.8	46.2	30.0
KL9	Kajala	590137	8964424	622	46.1	6.51	4625	-107	1045	60.2	64.2	31.9
IL1	Ilwalilo	583030	8970659	773	64.0	6.82	7084	-92	1630	74.5	39.0	15.0
IL2	Ilwalilo	582988	8970682	779	51.8	6.55	5139	-99	1186	55.0	49.0	19.0
IL3	Ilwalilo	582972	8970703	779	52.7	6.47	6088	-127	1472	63.1	42.5	15.2
IL4	Ilwalilo	583077	8970607	784	35.7	6.25	1615	-67	292	16.0	45.5	14.2
IL5	Ilwalilo	583052	8970636	779	53.8	6.52	5027	-80	1155	62	47.0	16.0
KJ1	Kiejo	584043	8976522	1457	21.2	4.92	115	5	14.5	5.9	4.4	1.90
KJ2	Kiejo	585057	8977403	1619	18.3	6.26	103	-4	12.4	5.6	4.7	1.85
KJ3	Kiejo	583884	8977141	1458	-	-	-	-	-	-	-	-
KJ4	Kiejo	584843	8976065	1473	20.8	4.78	78.7	31	8.6	4.2	3.4	1.60
SM1	Suma	577808	8977815	1242	24.0	7.35	342.8	-50	39.3	11.7	14.2	11.2
IG1	Igoma	572826	9004416	2318	17.6	6.68	76.0	-62	8.2	3.3	2.6	0.85
IG2	Igoma	573184	9004333	2330	14.9	7.30	83.4	-37	8.5	6.5	2.7	0.86
IG3	Igoma	585750	9001718	2756	15.1	6.85	58.7	-73	6.35	3.35	2.7	1.00

Code	Tot. Alk.	SO ₄	Cl	F	NO ₃	SiO ₂	Li	B	Fe	As	δ ¹⁸ O	δ ² H
	mg HCO ₃ /L	mg/L										‰ vs. VSMOW
KL1	2635	236	423	2.71	<0.05	128	0.70	0.89	0.48	0.18	-5.70	-27.0
KL2	2684	234	422	2.77	<0.05	128	0.67	0.89	0.64	0.19	-5.79	-27.2
KL3	2696	238	431	2.80	<0.05	126	0.70	0.92	0.40	0.20	-5.70	-27.4
KL4	2666	248	444	2.78	<0.05	130	0.71	0.95	0.55	0.20	-5.76	-27.5
KL5	2532	237	430	2.16	<0.05	137	0.70	0.94	0.78	0.21	-5.73	-27.7
KL6	2037	188	342	1.86	<0.05	102	0.55	0.73	0.010	0.14	-5.35	-25.3
KL8	2324	235	423	2.79	<0.05	117	0.65	0.89	0.042	0.19	-5.62	-27.2
KL9	2342	215	391	2.53	<0.05	113	0.60	0.83	0.010	0.16	-5.50	-26.3
IL1	3155	274	720	7.70	<0.05	89.2	0.95	1.37	0.047	0.30	-5.58	-30.1
IL2	2428	197	512	5.54	<0.05	73.0	0.65	0.98	0.006	0.18	-5.28	-27.4
IL3	2800	245	635	6.70	<0.05	85.3	0.85	1.23	0.020	0.27	-5.42	-28.5
IL4	753	53	122	1.85	<0.05	41.6	0.15	0.28	0.006	0.032	-	-
IL5	2358	191	506	5.56	<0.05	73.3	0.64	0.97	0.009	0.10	-5.25	-27.2
KJ1	75	0.6	1.1	0.18	1.2	45.7	<0.05	<0.05	0.004	<0.005	-4.79	-22.8
KJ2	71	0.3	0.62	0.18	<0.05	53.8	<0.05	<0.05	0.016	<0.005	-4.90	-24.1
KJ3	-	-	-	-	-	-	-	-	-	<0.005	-4.47	-20.9
KJ4	52	0.2	0.73	0.12	<0.05	47.6	<0.05	<0.05	0.004	<0.005	-4.61	-21.7
SM1	217	0.5	1.3	0.34	<0.05	61.8	<0.05	<0.05	0.322	<0.005	-4.77	-22.8
IG1	35	0.4	1.9	0.12	11.5	25.1	<0.05	<0.05	0.005	<0.005	-5.82	-32.1
IG2	43	0.7	1.2	0.13	11.6	27.5	<0.05	<0.05	0.147	0.005	-5.75	-32.0
IG3	43	0.3	0.35	0.15	0.3	26.5	<0.05	<0.05	0.006	<0.005	-6.35	-36.8

Table 1. Field data and results of the chemical and isotopic laboratory analyses of the water samples collected in the study area during this work.

Code	Place	Code	CO ₂	H ₂ S	N ₂	O ₂	Ar	He	H ₂	CH ₄	CO	δ ¹³ C-CO ₂
			μmol/mol									‰ vs. VPDB
KL-1	Kilambo	KL-1	989000	<100	200	85	9	<5	2	2.04	4	-5.46
KL-5	Kajala	KL-5	988000	<100	230	60	6	<5	2	1.64	4	-6.00
IL-3	Ilwalilo	IL-3	998000	<100	300	5	10	<5	10	12.0	2	-6.40

Table 2. Results of the chemical and isotopic laboratory analyses of the gas samples collected at Kilambo, Kajala and Ilwalilo during this work.

4. Water Geochemistry

4.1 Hydrochemical Classification

The triangular diagrams of major anions and major cations (Figure 2) indicate that the hot springs of Ilwalilo, Kilambo, and Kajala have Na-HCO₃ composition whereas cold springs and rivers have either Na-HCO₃ or Ca(Mg)-HCO₃ or Mg(Ca)-HCO₃ composition. Note that both diagrams were prepared starting from the concentrations in equivalent units, which are more suitable than weight units for the chemical classification of natural waters.

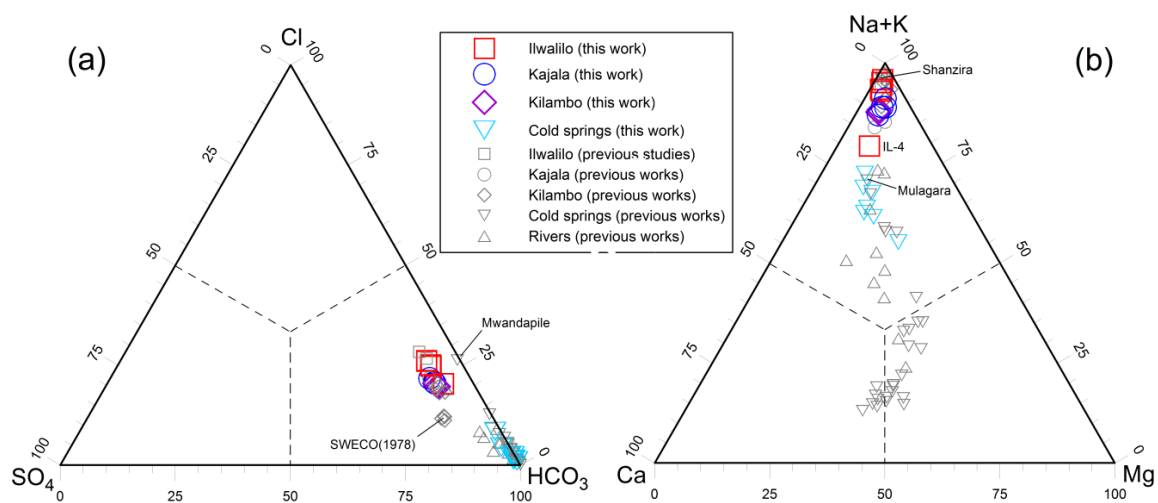


Figure 2: Triangular diagrams of (a) major anions and (b) major cations for the water samples collected in the study area during this work and previous studies.

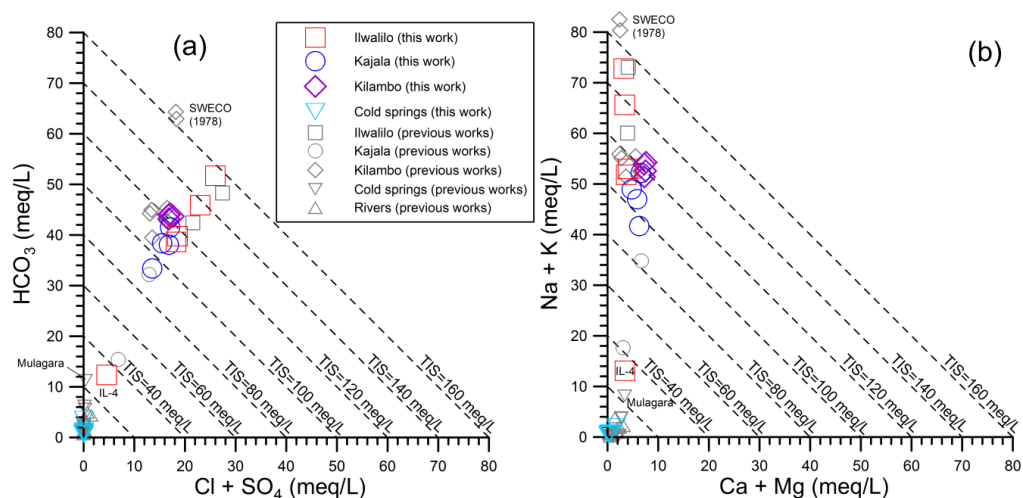


Figure 3: Correlation plots of (a) HCO₃ vs. SO₄ + Cl and (b) Na + K vs. Ca + Mg for the water samples collected in the study area during this work and previous studies.

The correlation plots of HCO_3 vs. $\text{Cl} + \text{SO}_4$ and $\text{Na} + \text{K}$ vs. $\text{Ca} + \text{Mg}$ (Figure 3) show that the Na-HCO_3 hot spring waters have relatively high Total Ionic Salinity (TIS), up to ~ 150 – 160 meq/L whereas cold springs and rivers have low TIS, generally lower than ~ 10 meq/L. Among the hot spring waters collected during this work, TIS varies from 33 to 154 meq/L at Ilwalilo, from 95 to 117 meq/L at Kajala, and from 119 to 123 meq/L at Kilambo, owing to the different extent of mixing between the deep thermal waters and cold shallow waters.

The hot spring waters of interest probably acquire their chemical characteristics through prolonged interaction of meteoric waters (as indicated by the $\delta^{18}\text{O}$ and $\delta^2\text{H}$ values of H_2O , see section 7) with basement rocks (mainly gneisses) sustained by conversion of CO_2 to HCO_3 .

4.2 Chloride Plots

The Cl plots of B and Li (Figure 4) show that the thermal waters of Kilambo and Kajala distribute along the same mixing line, with the Kilambo hot spring waters and the hottest Kajala sample, code KL-5, which have the highest Cl concentrations and are probably representative of the undiluted Kilambo-Kajala thermal endmember. In contrast, the thermal waters of Ilwalilo define a distinct mixing line, with the hottest sample, code IL-1, which has the highest Cl concentrations and probably represents the pure Ilwalilo thermal endmember. Moreover, the Cl concentration of sample IL1, 720 mg/L, is significantly higher than those of Kilambo waters (422–444 mg/L) and sample KL-5 from Kajala, 430 mg/L. B/Cl and Li/Cl ratios are somewhat higher at Kilambo-Kajala than at Ilwalilo. These observations suggest the presence of two separate thermal circuits, one discharging at Kilambo-Kajala, the other discharging at Ilwalilo.

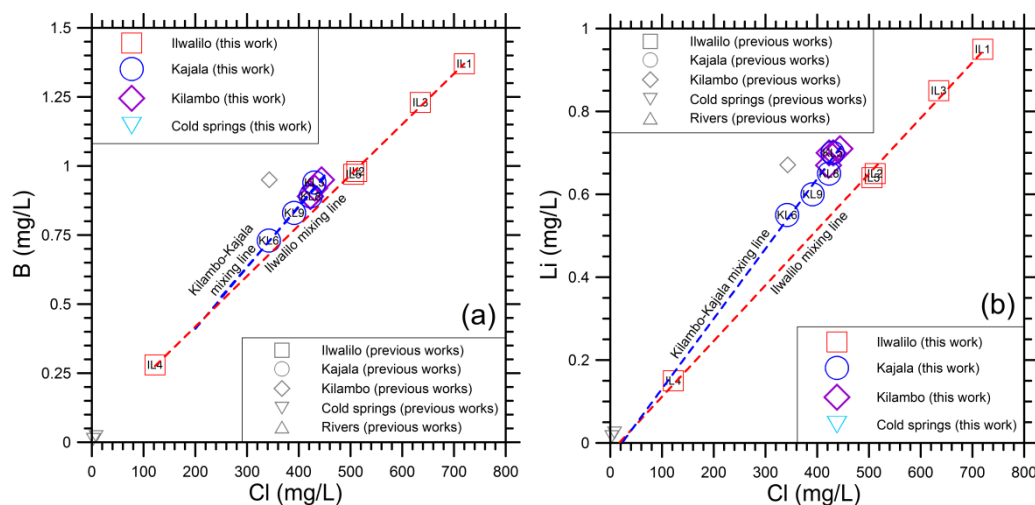


Figure 4: Chloride plots of (a) B and (b) Li for the water samples collected in the study area during this work and previous studies.

The Cl diagrams of alkalinity and SiO_2 (Figure 5), Na and K (Figure 6), SO_4 , and F (not shown) are similar to previous Cl plots. Again, two separate mixing lines are clearly recognizable, one for Kilambo-Kajala, the other for Ilwalilo, indicating that these solutes have mobile or close to mobile behaviour and that the effects of gain/loss of these chemical components, through mineral dissolution/precipitation and desorption from/adsorption onto solid surfaces, are negligible. Therefore, Na, K, and SiO_2 concentrations of the thermal endmembers are presumably representative of reservoir conditions and can be safely used in geothermometric applications.

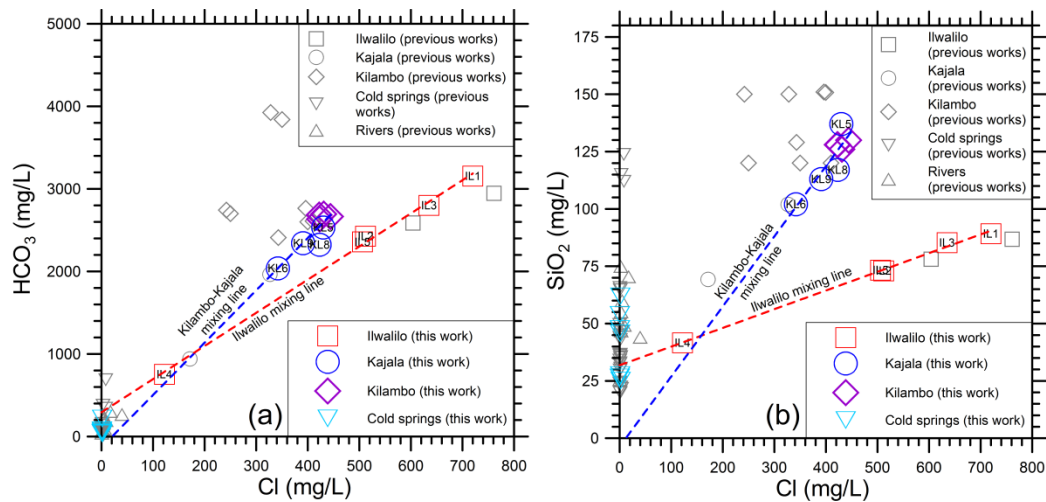


Figure 5: Chloride plots of (a) alkalinity and (b) SiO_2 for the water samples collected in the study area during this work and previous studies.

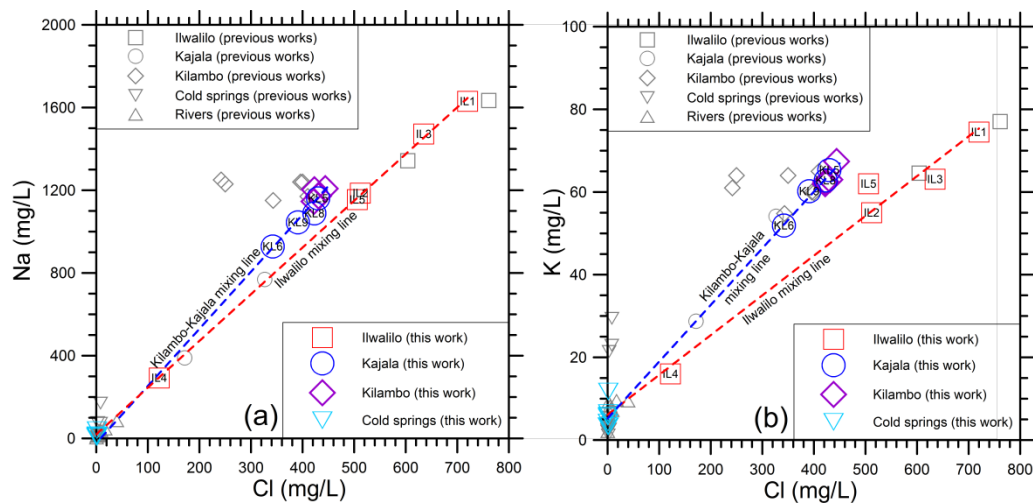


Figure 6: Chloride plots of (a) Na and (b) K for the water samples collected in the study area during this work and previous studies.

In contrast, in the Cl plots of Ca and Mg (Figure 7), the Kilambo-Kajala mixing line is not recognizable owing to loss of both Mg and Ca. Hence, the Ca concentration of the Kilambo-Kajala thermal endmember was obtained from speciation-saturation calculations assuming equilibrium with calcite under reservoir conditions whereas its Mg concentration was computed from the K-Mg geothermometer imposing the equilibrium temperature. If the computed Ca and Mg concentrations of the Kilambo-Kajala thermal endmember are correct, it follows that the thermal water acquires Ca and Mg during its upflow towards the surface discharge points under comparatively high P_{CO_2} values. Afterwards, occurrence of CO_2 separation, probably at the surface or relatively close to it, triggers precipitation of calcite and loss not only of Ca but also of Mg, which is readily incorporated in precipitating calcite.

The Ilwalilo thermal endmember has probably gained Ca only, during the uprise towards the surface under relatively high P_{CO_2} values, since the K-Mg temperature of sample IL-1 is consistent with its SiO_2 (quartz/chalcedony) temperature (see section 5). Again, the initial Ca concentration was obtained from speciation-saturation calculations assuming saturation with calcite under reservoir conditions.

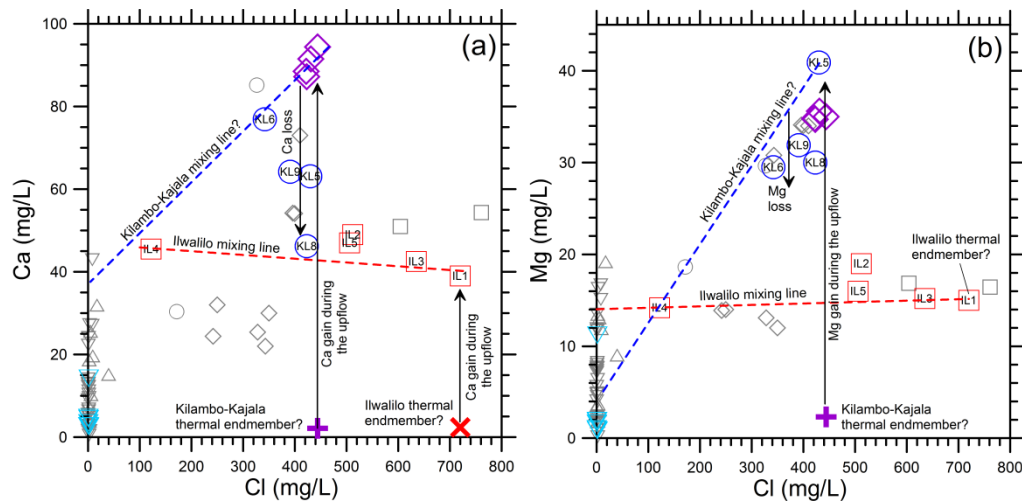


Figure 7: Chloride plots of (a) Ca and (b) Mg for the water samples collected in the study area during this work and previous studies. Symbols as in previous figures.

5. Water Geothermometers

Sample IL-1, which is possibly representative of the pure Ilwalilo thermal endmember (being the one not affected or least affected by mixing), has no-steam-loss SiO_2 (quartz/chalcedony) temperature (Giggenbach et al., 1994) of 112 °C. This value is very similar to the K-Mg temperature (Giggenbach, 1988), 113 °C, whereas Na-K temperatures, 177 °C (Giggenbach, 1988) or 158 °C (Fournier, 1979), are probably meaningless. In fact, Na-K temperatures are not controlled by overall K-feldspar/albite/aqueous solution equilibrium but by the condition of equality of the saturation indices (SI) of K-feldspar and albite, which are both $\neq 0$, at a temperature intermediate between those indicated by Na-K geothermometers, as shown by the SI vs. temperature plot (Figure 8a). This plot also points out that the Ilwalilo geothermal liquid attains saturation with chalcedony, albite, K-feldspar, illite, clinocllore-7A, and calcite in the temperature interval 100-112 °C and with quartz at ~130 °C, in accordance with the SiO_2 and K-Mg temperatures.

Samples KL-1, KL-2, KL-3, KL-4, and KL-5, which are possibly representative of the pure Kilambo-Kajala thermal endmember (being the ones not affected or least affected by mixing), have no-steam-loss SiO_2 (quartz/chalcedony) temperature (Giggenbach et al., 1994) of 137 ± 2 °C. The K-Mg temperature, 96 ± 1 °C, probably underestimates the equilibrium temperature due to Mg acquisition upon cooling (see above). Again, Na-K temperatures, 188 ± 2 °C (Giggenbach, 1988) or 170 ± 2 °C (Fournier, 1979), have probably no meaning, because they are governed by the condition $\text{SI}_{\text{K-feldspar}} = \text{SI}_{\text{albite}} \neq 0$, at a temperature intermediate between those indicated by Na-K geothermometers, instead of overall K-feldspar/albite/aqueous solution equilibrium, as shown by the SI vs. temperature plot (Figure 8b). This plot also highlights that the Kilambo-Kajala geothermal liquid attains equilibrium with chalcedony, albite, K-feldspar, illite, clinocllore-7A, and calcite in the temperature range 125-137 °C and with quartz at ~150 °C, in agreement with the SiO_2 temperature.

Therefore, the most probable reservoir temperatures are considered to be 135-139 °C for the Kilambo-Kajala thermal circuit and 112-113 °C for the Ilwalilo thermal circuit.

The P_{CO_2} of the reservoir liquid is 1.19 bar for Ilwalilo and 1.74 ± 0.03 bar for Kilambo-Kajala as pointed out by the K-Ca P_{CO_2} -indicator of Giggenbach (1988). These P_{CO_2} values are two orders of magnitude higher than the “full equilibrium P_{CO_2} ” values, 0.013 bar and

0.033 ± 0.003 bar, respectively, implying that calcite is stable under reservoir conditions instead of Ca-Al-silicate minerals and that P_{CO_2} is an externally fixed parameter. This means that a continuous flux of CO_2 -rich deep gases occurs through the two geothermal systems in the same manner as the heat flux. This inference is supported by the $\delta^{13}C$ values of CO_2 , -5.5 to -6.0 ‰ at Kilambo-Kajala and -5.6 to -6.4 ‰ at Ilwalilo (see Table 2 and data of Kraml et al., 2008, Delalande et al., 2011, Ochmann and Garofalo, 2013, and Barry et al., 2013), suggesting that CO_2 is mainly contributed by deep sources, such as degassing of hydrothermal-magmatic systems, mantle degassing, or other processes occurring at depth.

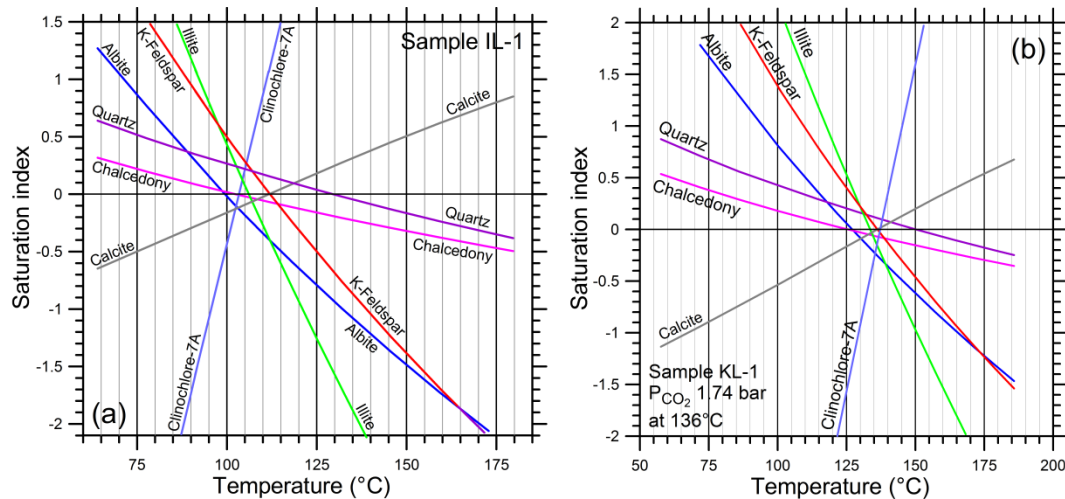


Figure 8: Saturation indices vs. temperature plots for (a) sample IL-1 from Ilwalilo and (b) sample KL-1 from Kilambo, based on recalculated Mg, Ca, and DIC concentrations.

6. Gas chemistry and Geothermometry

Table 2 and data from previous works (Kraml et al., 2008, Ochmann and Garofalo, 2013, de Moor et al., 2013) show that the free gases discharged from the hot springs of Kilambo, Kajala and Ilwalilo are extremely rich in CO_2 and exceptionally poor in reduced gas species (H_2S , CH_4 , H_2 and CO) and He. Nitrogen is the second most abundant gas constituent after CO_2 . The Ar/N_2 ratios, 22 to 38, are similar to or somewhat lower than the air-saturated water values, 39 to 45 from 25 to 100 °C.

The cold gas vents of Ikama and Kiejo have $^3He/^4He$ isotopic ratios of 6.1 to 7.4 R_A , typical of gases of direct mantle provenance, whereas Kilambo hot springs have $^3He/^4He$ isotopic values of 1.0 to 3.7 R_A , due to mixing between mantle gases enriched in 3He and crustal gases enriched in 4He , as already noted by Pik et al. (2006) and Barry et al. (2013). This implies that probably there is no relation between the gas vents and the thermal circuits of the prospect area, in spite of the lack of He isotope data for Lufundo and Ilwalilo.

Assuming that H_2 equilibrates in a single liquid phase at R_H of -2.82, H_2 -Ar- and H_2 - N_2 -temperatures of ~140-150 °C are computed for samples KL-1 from Kilambo and KL-5 from Kajala, in agreement with those indicated by the SiO_2 geothermometer and the SI vs. temperature plot (see section 5). Sample IL-3 from the Ilwalilo has H_2 -Ar- and H_2 - N_2 -temperatures of ~180-190 °C, which are significantly higher than those given by the SiO_2 and K-Mg geothermometers and the SI vs. temperature plot (see section 5). It is possible that H_2 was not able to readjust at the low temperatures of the Ilwalilo thermal circuit, due to the slow kinetics of relevant reactions. If so, the H_2 -Ar- and H_2 - N_2 - temperatures might be present at higher depths (below the Ilwalilo thermal circuit) or might be meaningless.

7. The $\delta^2\text{H}$ and $\delta^{18}\text{O}$ Values of H_2O

In the correlation diagram of $\delta^2\text{H}$ vs. $\delta^{18}\text{O}$ (Figure 9), available isotope data for the hot springs of Ilwalilo, Kilambo and Kajala, and for the cold springs and rivers of nearby areas (from this work and previous studies) are compared with three meteoric water lines (MWLs), namely the worldwide MWL, the regional MWL (Bergonzini et al., 2001), and the local MWL, which was obtained through linear fit of the isotope values of the cold springs sampled in this work ($N = 8$; $R^2 = 0.997$):

$$\delta^2\text{H} = 8.74 \cdot \delta^{18}\text{O} + 18.65. \quad (1)$$

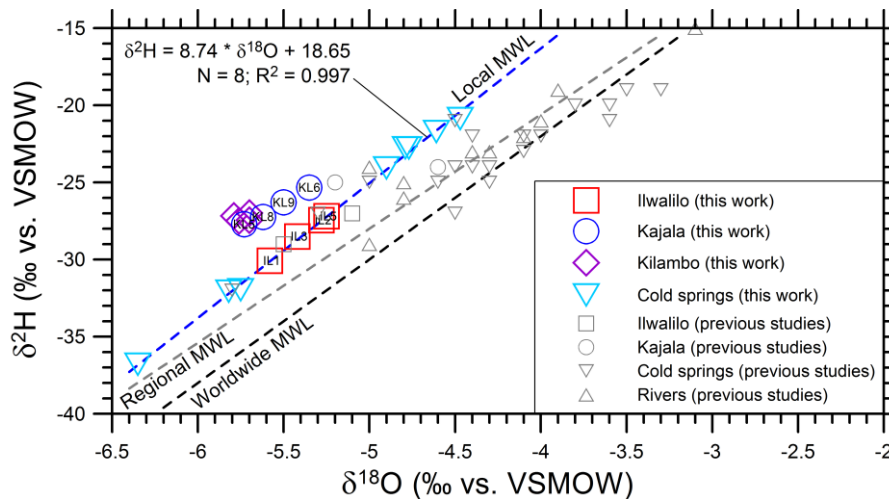


Figure 9: Correlation diagram of $\delta^2\text{H}$ vs. $\delta^{18}\text{O}$ for the water samples collected from the hot springs of Ilwalilo, Kilambo and Kajala, as well as from cold springs and rivers of nearby areas surveyed during this work and previous studies. Also shown are the worldwide MWL, the regional MWL (Bergonzini et al., 2001), and the local MWL.

Most cold springs and rivers from previous studies distribute between the local MWL and the worldwide MWL, possibly due to occurrence of evaporation processes and/or provenance of atmospheric vapor masses from different sources. In contrast, the cold springs sampled during this work are certainly not affected by evaporation processes and related atmospheric vapor masses seem to come from a single source which is different from the oceanic source.

The Ilwalilo hot spring waters are positioned along the local MWL and are, therefore, of meteoric origin. Sample IL-1, which is the least affected by mixing and is probably representative of the pure thermal endmember (see above), is isotopically lighter than other Ilwalilo hot spring waters, indicating that the pure Ilwalilo thermal endmember is isotopically much lighter than the local cold endmember.

The Kilambo-Kajala hot spring waters are positioned to the left of the local MWL, showing a negative oxygen shift, which is probably due to exchange of oxygen isotopes between H_2O and CO_2 , as already suggested by Kraml et al. (2012). Nevertheless, also these hot spring waters are of meteoric origin. Samples KL-1, KL-2, KL-3, KL-4, and KL-5, which are those least influenced by mixing and are probably representative of the pure thermal endmember (see above), are isotopically lighter than other Kilambo-Kajala hot spring waters. Hence, also the pure Kilambo-Kajala thermal endmember is isotopically much lighter than the local cold endmember.

The different isotope values of thermal endmembers and cold endmembers (at least the $\delta^2\text{H}$ value of the Kilambo-Kajala thermal endmember, because its $\delta^{18}\text{O}$ value is affected by

exchange of oxygen isotopes between H₂O and CO₂) reflect different infiltration elevations, which can be evaluated using the following two relations (H is elevation in m asl):

$$H = -82.17 \cdot \delta^2\text{H} - 290.9 \quad (2)$$

$$H = -704.7 \cdot \delta^{18}\text{O} - 1740.7. \quad (3)$$

These relations were reconstructed adopting the small spring method (Vespasiano et al., 2015) based on the isotope characteristics of the cold springs sampled during this work. Equations (2) and (3) provide an average infiltration elevation of 2186 ± 5 m asl for sample IL-1 from Ilwalilo, whereas equation (2) gives an average infiltration elevation of 1957 ± 23 m asl for samples KL-1, KL-2, KL-3, and KL-4 from Kilambo and KL-5 from Kajala.

8. Contribution to the Elaboration of the Conceptual Models of the Two Thermal Circuits

The interpretation and synthesis of the geochemical data available for the Kiejo-Mbaka prospect area, produced during this work and previous studies, suggest that the hot springs of Kilambo and Kajala represent the surface discharge of the a unique fault-controlled geothermal circuit, whereas the hot springs of Ilwalilo are the outflow of a distinct fault-controlled geothermal circuit. Due to their similarity, a single description is given here below for the two geothermal circuits.

In the recharge area, situated at ~2190 m asl for Ilwalilo and ~1960 m asl for Kilambo-Kajala, infiltrating meteoric waters are conveyed downward along either one or more NW-SE-trending tectonic structures dissecting the Livingstone escarpment and descend slowly to considerable depths. After this sub-vertical downward movement, the meteoric waters, somewhat heated up through conductive rock-to-water heat transfer, flow slightly up dip due to buoyancy effects moving southwestwards along fault-controlled permeable zones.

Along its southwestward travel, water undergoes chemical changes sustained by a nearly continuous supply of CO₂-rich deep gases, extracts further heat from rocks, and finally approaches or achieves the condition of thermo-chemical equilibrium with the basement rocks at temperatures of 112-113°C for Ilwalilo and 135-139°C Kilambo-Kajala. Assuming that the local geothermal gradient is 66°C km⁻¹, that is twice the shallow adiabatic geothermal gradient of 33°C km⁻¹, these temperatures are expected to occur at depths in the order of 1.3 km below Ilwalilo and 1.7 km below Kilambo-Kajala.

Then, the thermal water experiences a relatively quick uprise towards the surface, moving along the Mbaka fault. In its travel along the uprising leg of the thermal circuit, the thermal water experiences a substantial temperature decrease and acquires Ca (both below Kilambo-Kajala and Ilwalilo) and Mg (below Kilambo-Kajala only) through rock leaching under high P_{CO2} conditions. Then, at shallow depth, CO₂ exsolution occurs, triggering calcite precipitation. Mixing with shallow cold waters takes place locally.

REFERENCES

- Barry, P.H., Hilton, D.R., Fischer, T.P., de Moor, J.M., Mangasini, F., and Ramirez, C. "Helium and carbon isotope systematics of cold "mazuku" CO₂ vents and hydrothermal gases and fluids from Rungwe Volcanic Province, southern Tanzania." *Chem. Geol.*, 339, (2012), 141-156.

- Bergonzini, L., Gibert, E., Winckel, A., and Merdaci, O. “Bilans hydrologique et isotopique (^{18}O et ^2H) du lac Massoko, Tanzanie. Quantification des échanges lac-eaux souterraines.” *C. R. Acad. Sci. Paris, Sciences de la Terre et des Planètes*, 333, (2001), 617–623.
- Delalande, M., Bergonzini, L., Gherardi, F., Guidi, M., Andre, L., Abdallah, I., and Williamson, D. “Fluid geochemistry of natural manifestations from the southern Poroto-Rungwe hydrothermal system (Tanzania): preliminary conceptual model.” *J. Volcanol. Geotherm. Res.*, 199, (2011), 127–141.
- De Moor, J.M., Fischer, T.P., Sharp, Z.D., Hilton, D.R., Barry, P.H., Mangasini, F., and Ramirez, C. “Gas chemistry and nitrogen isotope compositions of cold mantle gases from Rungwe Volcanic Province, southern Tanzania.” *Chem. Geol.*, 339, (2013), 30–42.
- Fournier, R.O. “A revised equation for the Na/K geothermometer.” *Geotherm. Res. Counc. Trans.*, 5, (1979)1-16.
- Giggenbach, W.F. “Geothermal solute equilibria. Derivation of Na-K-Mg-Ca geoindicators.” *Geochim. Cosmochim. Acta*, 52, (1988), 2749-2765.
- Giggenbach, W.F., Sheppard, D.S., Robinson, B.W., Stewart, M.K., and Lyon, G.L. “Geochemical structure and position of the Waiotapu geothermal field, New Zealand.” *Geothermics*, 23, (1994), 599-644.
- Kraml, M., Schaumann, G., Kalberkamp, U., Stadtler, C., Delvaux, D., Ndonde, P.B., Mnjokava, T.T., Chiragwile, S.A., Mayalla, J.W., Kabaka, K., Mwano, J.M., Makene, C. “Geothermal Energy as an Alternative Source of Energy for Tanzania.” Final Technical Report of Phase I (2006-2009), GEOTHERM-Project 2002.2061.6, (2008), 235 pp.
- Kraml, M., Kreuter, H., Robertson, G., and Mbaka exploration team members. “Small-scale rural electrification and direct use of low-temperature geothermal resources at Mbaka Fault in SW Tanzania.” *Proceedings: 4th African Rift Geothermal Conference*, Nairobi, Kenya (2012), 11 pp.
- Makundi, J.S., and Kifua, G.M. “Geothermal features of the Mbeya prospect in Tanzania.” *Geotherm. Res. Counc. Trans.*, 9, (1985), 451–454.
- Ochmann, N., and Garofalo, K. “Geothermal Energy as an Alternative Source of Energy for Tanzania.” Final Technical Report of Phase II (2010-2013), GEOTHERM-Project 2002.2061.6, (2013), 156 pp.
- Pik, R., Marty, B., and Hilton, D.R. “How many mantle plumes in Africa? The geochemical point of view.” *Chem. Geol.*, 226, (2006), 100–114.
- Principe, C., Pasqua, C., and Pisani, P. “Surface exploration and training in Luhoi and Kiejo-Mbaka geothermal areas, Tanzania. Geological survey report – Kiejo” Report prepared by ELC-Electroconsult for TGDC-Tanzania Geothermal Development Company Limited, (2017), 50 pp.
- SWECO. “Reconnaissance of Geothermal Resources.” Report for the Ministry of Water, Energy and Minerals of Tanzania, (1978), 51pp.
- Vespasiano, G., Apollaro, C., De Rosa, R., Muto, F., Larosa, S., Fiebig, J., Mulch, A., and Marini, L. “The Small Spring Method (SSM) for the definition of stable isotope–elevation relationships in Northern Calabria (Southern Italy).” *Appl. Geochem.*, 63, (2015), 333-346.